

RELAXATION SCHEMES FOR THE M_1 MODEL WITH SPACE-DEPENDENT FLUX: APPLICATION TO RADIOTHERAPY DOSE CALCULATION

Teddy Pichard and Martin Frank

Mathematics division, Center for Computational Engineering Science, Rheinisch-Westfälische Technische Hochschule

Schinkelstrasse 2, Aachen, 52062-52080, Germany

pichard@celia.u-bordeaux1.fr; frank@mathcces.rwth-aachen.de

Denise Aregba-Driollet, Stéphane Brull, and Bruno Dubroca

Institut de Mathématiques de Bordeaux, Université de Bordeaux

351 cours de la libération, Talence, 33400, France

denise.aregba@math.u-bordeaux1.fr; stephane.brull@math.u-bordeaux1.fr;

bruno.dubroca@math.u-bordeaux1.fr

ABSTRACT

Because of stability constraints, most numerical schemes applied to hyperbolic systems of equations turn out to be costly when the flux term is multiplied by some very large scalar. This problem emerges with the M_1 system of equations in the field of radiotherapy when considering heterogeneous media with very disparate densities. Additionally, the flux term of the M_1 system is non-linear, and in order for the model to be well-posed the numerical solution needs to fulfill conditions called realizability. In this paper, we propose a numerical method that overcomes the stability constraint and preserves the realizability property. For this purpose, we relax the M_1 system to obtain a linear flux term. Then we extend the stencil of the difference quotient to obtain stability. The scheme is applied to a radiotherapy dose calculation example.

Key Words: Radiotherapy, Moments models, relaxation models, method of characteristics

1 INTRODUCTION

The present work is devoted to the numerical solution of a moment system of equations, which describes the transport of electrons in tissues. The model finds application in the field of radiotherapy dose calculation when considering low density media ([1]):

$$\frac{1}{\rho(x)} \nabla_x \cdot \psi^1(x, \epsilon) = \partial_\epsilon (S(\epsilon) \psi^0)(x, \epsilon), \quad (1a)$$

$$\frac{1}{\rho(x)} \nabla_x \cdot \psi^2(x, \epsilon) = \partial_\epsilon (S(\epsilon) \psi^1)(x, \epsilon) - 2T(\epsilon) \psi^1(x, \epsilon), \quad (1b)$$

where the unknowns $\psi^0 \in \mathbb{R}$, $\psi^1 \in \mathbb{R}^3$ and $\psi^2 \in \mathbb{R}^{3 \times 3}$ depend on energy $\epsilon \in \mathbb{R}^+$ and position $x \in \mathbb{R}^3$. The stopping power S and the transport coefficient T are positive functions of ϵ

characterizing the loss of energy and the deflection of the electrons during their transport. Finally, $\rho(x) > 0$ is the density of the medium at point x . This equation is solved by marching backward in energy, i.e. we prescribe $\psi^0(\epsilon_{\max}, x) = 0$ and $\psi^1(\epsilon_{\max}, x) = 0_{\mathbb{R}^3}$ at initial energy ϵ_{\max} (which means that electrons have bounded energy) and we solve (1) from ϵ_{\max} to 0.

1.1 M_1 model

The system (1) is composed of 4 equations with 9 unknowns (scalar ψ^0 , vector ψ^1 and symmetric matrix with known trace ψ^2). It is closed using the entropy minimization principle ([2]):

$$\begin{aligned} & \text{We seek the function } \psi_M \geq 0 \text{ minimizing the Boltzmann entropy } H(f) = \int_{S^2} f \ln(f) d\Omega \\ \psi_M = \underset{f \in \mathcal{F}_1}{\operatorname{argmin}} H(f) \quad & \text{with } \mathcal{F}_1 = \left\{ f \geq 0 \text{ s.t. } \int_{S^2} f d\Omega = f^0, \text{ and } \int_{S^2} \Omega f d\Omega = f^1 \right\}. \end{aligned} \quad (2)$$

We close the system (1) by fixing ψ^2 as the 2nd order moment of ψ_M

$$\psi^2 = \int_{S^2} \Omega \Omega^T \psi_M(\Omega). \quad (3)$$

System (1) with this closure is called M_1 model. The M_1 model is closely related to some underlying kinetic model because the function ψ_M given by (2) is known to be the most probable kinetic distribution function realizing the first two moments ([3, 4]). This choice of closure provides several desirable properties such as hyperbolicity of (1) and entropy dissipation ([2]).

Moment models are a good compromise between full kinetic models, precise but numerically costly, and diffusion models, not able to represent some physical phenomena.

The M_1 model is valid under a condition on ψ^0 and ψ^1 . Indeed, the M_1 closure exists only if there exists such a non-negative function ψ_M . This requirement is called realizability condition. A special attention is needed for this condition when developing numerical schemes for (1). We define the set \mathcal{A}_1 of realizable moments by

$$(\psi^0, \psi^1) \in \mathcal{A}_1 \Leftrightarrow \exists f \geq 0, \text{ s.t. } \int_{S^2} f(\Omega) d\Omega = \psi^0, \int_{S^2} \Omega f(\Omega) d\Omega = \psi^1. \quad (4)$$

Note that \mathcal{A}_1 is a convex cone. Numerical schemes applied to the system (1) need to preserve the realizability property.

For the M_1 model, the realizability property can be characterized by ([5])

$$\mathcal{A}_1 = \{(0, 0_{\mathbb{R}^3})\} \cup \left\{ (\psi^0, \psi^1) \in \mathbb{R}^{*+} \times \mathbb{R}^3 \text{ s.t. } \frac{|\psi^1|}{\psi^0} < 1 \right\}. \quad (5)$$

If $(\psi^0, \psi^1) \in \mathcal{A}_1$ one can compute the closure. By geometrical considerations ([6]),

$$\psi^2 = \psi^0 \left(\frac{3\chi - 1}{2} \frac{\psi^1}{|\psi^1|} \otimes \frac{\psi^1}{|\psi^1|} + \frac{1 - \chi}{2} Id_{\mathbb{R}^{3 \times 3}} \right), \quad (6)$$

where χ is the Eddington factor and depends only on $|\psi^1|/\psi^0 \in [0, 1]$.

1.2 Problem statement

In radiotherapy, the studied electrons may be transported through strongly heterogeneous media, e.g. $\rho = 1$ in water and $\rho = 10^{-3}$ in air. Standard numerical schemes applied to (1) require a very small energy step $\Delta\epsilon$ to converge, which prevents these schemes from being usable for practical application. To see this, consider a one dimensional problem. In slab geometry, (1) can be reduced into

$$\frac{1}{\rho(x)} \partial_x \psi^1(x, \epsilon) = \partial_\epsilon (S(\epsilon) \psi^0)(x, \epsilon), \quad (7a)$$

$$\frac{1}{\rho(x)} \partial_x \psi^2(x, \epsilon) = \partial_\epsilon (S(\epsilon) \psi^1)(x, \epsilon) - 2T(\epsilon) \psi^1(x, \epsilon), \quad (7b)$$

where ψ^i are now scalars and $x \in \mathbb{R}$. The previous closure in 1D simply reads

$$\psi^2 = \psi^0 \chi(|\psi^1|/\psi^0). \quad (8)$$

To shorten notation, 1D system (7) is rewritten

$$\partial_\epsilon (S(\epsilon) \bar{\psi}) - \frac{1}{\rho(x)} \partial_x \bar{F}(x, \epsilon) + T(\epsilon) L \bar{\psi} = 0, \quad (9)$$

where $\bar{\psi} = (\psi^0, \psi^1)^T$, $\bar{F} = (\psi^1, \psi^2)^T$ and $L = \begin{pmatrix} 0 & 0 \\ 0 & 2 \end{pmatrix}$. The superscript $\bar{\cdot}$ refers to vectors.

As a first approach, we use an HLL scheme ([7]) to solve the 1D moment system (7).

$$S^{n+1} \bar{\psi}_l^{n+1} = \left[S^n \bar{\psi}_l^n - \frac{\Delta\epsilon^n}{\rho_l \Delta x} \left(\bar{G}_{l+\frac{1}{2}}^n - \bar{G}_{l-\frac{1}{2}}^n \right) + T^n L \bar{\psi}_l^n \right], \quad (10)$$

with

$$\bar{G}_{l+\frac{1}{2}}^n = \frac{1}{2} (\bar{F}_{l+1}^n + \bar{F}_l^n - (\bar{\psi}_{l+1}^n - \bar{\psi}_l^n)). \quad (11)$$

The subscript l refers to the position x and n to the energy ϵ . This scheme is stable under a Courant Friedrichs Lewy (CFL) condition

$$\Delta\epsilon^n \leq S^n \left(\frac{1}{\min(\rho_l) \Delta x} + 2T^n \right)^{-1}. \quad (12)$$

In practice, the density ρ is inhomogeneous and can have very strong variations. Then $\min(\rho_l)$ might be very low, and the numerical scheme requires very small $\Delta\epsilon^n$.

This problem was investigated in [8] and solved by modifying the grid in one space dimension. The generalization to multi-dimensional (multi-D) problems was not straight-forward, but introduced additional splitting errors. In the present paper, we propose a numerical approach ensuring the realizability that does not constrain the energy step, independent of the grid, and which works for multi-D problems. In Section 2, we describe the numerical approach which consists of two parts. First, we use a relaxation model to obtain a linear flux term. Second, we construct numerical schemes for linear hyperbolic equations with spatially varying flux that are unconditionally stable. The last section is devoted to the validation of the numerical approach on a relevant test case.

2 NUMERICAL APPROACH

We write the multi-D system (1) in the form

$$\partial_\epsilon(S(\epsilon)\bar{\psi}) - \frac{1}{\rho(x)}\nabla_x \cdot \bar{F}(x, \epsilon) + T(\epsilon)L \cdot \bar{\psi} = 0, \quad (13)$$

with $L = \begin{pmatrix} 0 & 0_{\mathbb{R}^3} \\ 0_{\mathbb{R}^3}^T & 2Id_{\mathbb{R}^3 \times 3} \end{pmatrix}$. Here $\bar{\psi} = (\psi^0, \psi^1)^T \in \mathbb{R}^4$ and $\bar{F} = (\psi^1, \psi^2) \in \mathbb{R}^{3 \times 4}$. The superscript $\bar{\cdot}$ refers to vectors of vectors, i.e. matrices. Note that the divergence operator $\nabla_x \cdot (\cdot)$ is applied separately to each vector component $\psi^1 \in \mathbb{R}^3$ and $\psi_{i,:}^2 \in \mathbb{R}^3$ composing $\bar{F} = (\psi^1, \psi_{1,:}^2, \psi_{2,:}^2, \psi_{3,:}^2)$.

2.1 Relaxation schemes for moment equations

We use a relaxation approximation of the system (13) (afterward called AN after [9, 10]) described in [9, 11] for hyperbolic systems of equations and completed for parabolic systems in [10, 12]. Special focus will be put on the preservation of the realizability domain.

2.1.1 Principle

We recall the principle of AN relaxation. Let us choose J relaxation vectors $(\bar{\lambda}_j)_{j=1,\dots,J} \in \mathbb{R}^3$. We associate to each of them a set of moments $(\bar{f}_j^\tau)_{j=1,\dots,J} \in \mathbb{R}^4$ depending on a relaxation parameter τ and a set of Maxwellians $(\bar{M}_j^\tau)_{j=1,\dots,J} \in \mathbb{R}^4$. Each set \bar{f}_j^τ or \bar{M}_j^τ correspond to a set of moments $\bar{\psi} = (\psi^0, \psi^1) \in \mathbb{R}^4$. The Maxwellians are linked to the original moments (13) through the consistency conditions

$$\sum_j \bar{M}_j^\tau = \bar{\psi} \quad \text{and} \quad \sum_j \bar{\lambda}_j \otimes \bar{M}_j^\tau = \bar{F}(\bar{\psi}), \quad (14)$$

where \otimes is the tensor product. In this study, we choose realizable Maxwellians, i.e.

$$\forall j = \{1, J\}, \quad \bar{M}_j^\tau(\bar{\psi}) \in \mathcal{A}_1 \quad \text{whenever} \quad \bar{\psi} \in \mathcal{A}_1. \quad (15)$$

The following system of equations is a relaxation system for (13)

$$\rho \partial_\epsilon(S \bar{f}_j^\tau) - \bar{\lambda}_j \cdot \nabla_x \bar{f}_j^\tau + \rho L \cdot \bar{f}_j^\tau = \frac{1}{\tau} \left(\bar{M}_j^\tau \left(\sum_k \bar{f}_k^\tau \right) - \bar{f}_j^\tau \right), \quad 1 \leq j \leq J. \quad (16)$$

The solutions \bar{f}_j^0 of the limit problem ($\tau \rightarrow 0$) correspond to the desired solution of the original system (13). Formally, multiplying (16) by τ and $\tau \rightarrow 0$ leads to

$$\bar{M}_j^0 \left(\sum_k \bar{f}_k^0 \right) = \bar{f}_j^0.$$

Then replacing \bar{f}_j^0 by \bar{M}_j^0 in (16) and summing the equations reads

$$\rho \partial_\epsilon (S \sum_j \bar{M}_j^0) - \nabla_x \cdot (\sum_j \bar{\lambda}_j \otimes \bar{M}_j^0) + \rho L \cdot (\sum_j \bar{M}_j^0) = 0,$$

which is exactly (13).

As we only want to solve the limit system for $\tau \rightarrow 0$, the index τ is removed in the rest of this paper. The upper index n now refers to energy step ϵ^n , first lower index j to relaxation speed $\bar{\lambda}_j$ and second lower index l to position x_l . Note that the spatial fluxes of the relaxed system are linear even if the ones from the original system are not.

In 1D, it is a well-known stability requirement ([10, 11, 13]) that all eigenvalues of $\partial_{\bar{\psi}} \bar{F}(\bar{\psi})$ have to be bounded by the extremal relaxation speed. For our problem, this condition can be written

$$\text{Spectrum} \left(\partial_{\bar{\psi}} (\bar{F}(\bar{\psi}) \cdot e_i) \right) \subset [\min_j \bar{\lambda}_j \cdot e_i, \max_j \bar{\lambda}_j \cdot e_i]. \quad (17)$$

Note that we can rewrite

$$\partial_{\bar{\psi}} (\bar{F}(\bar{\psi}) \cdot e_i) = \frac{\partial(\psi_i^1, \psi_{i,1}^2, \psi_{i,2}^2, \psi_{i,3}^2)}{\partial(\psi^0, \psi_1^1, \psi_2^1, \psi_3^1)}.$$

Simple computations (see e.g. [14]) leads to write $\text{Spectrum} \left(\partial_{\bar{\psi}} (\bar{F}(\bar{\psi}) \cdot e_i) \right) \subset [-1, 1]$ for $i \in \{1, 3\}$.

In practice, the solution of (13) is obtained as follow:

- We initialize $\bar{f}_j^0 := \bar{M}_j^0(\bar{\psi}^0)$ at the energy step ϵ^0 .
- We define intermediate states $\bar{f}_j^{n+\frac{1}{2}}$ by solving the homogeneous equations

$$\partial_\epsilon (S \bar{f}_j) - \frac{\bar{\lambda}_j}{\rho} \cdot \nabla_x \bar{f}_j + L \cdot \bar{f}_j = 0, \quad 1 \leq j \leq 2. \quad (18)$$

We discretize the term $L \cdot \bar{f}_j$ implicitly (this choice is explained in the following). The spatial derivative is approximated by some finite difference formula (to be specified later) which leads to

$$S^{n+1} \bar{f}_{jl}^{n+\frac{1}{2}} = S^n (C_j \bar{f}_j^n)_l + \Delta \epsilon^n T^{n+1} L \cdot \bar{f}_{jl}^{n+\frac{1}{2}}, \quad (19)$$

where $C_j \bar{f}_j^n$ is a convex combination of values of \bar{f}_j^n (see below remark 2).

- Then the solution is corrected by solving the rest of the equation, which, for $\tau \rightarrow 0$, corresponds to taking $\bar{M}_j^{n+1} := \bar{f}_j^{n+\frac{1}{2}}$.
- The solution at new energy is computed as

$$\bar{\psi}^{n+1} := \sum_j \bar{M}_j^{n+1}. \quad (20)$$

2.1.2 Realizability

This method preserves the realizability property from an energy step to the next one:

Proposition 1. *If for all l , we have $\bar{\psi}_l^n \in \mathcal{A}_1$ at energy step ϵ^n then the solution $\bar{\psi}_l^{n+1}$ obtained by solving the relaxed system (16) with the scheme (19) is also in \mathcal{A}_1 at energy step ϵ^{n+1} for all l .*

Proof. The realizability of $\bar{\psi}^{n+1}$ is obtained via (20) through the realizability of \bar{M}_j^{n+1} . First, we initialize \bar{f}_j^n at energy ϵ^n such that. Second, we show by induction that $\bar{f}_j^{n+\frac{1}{2}}$ is realizable at the new energy step. Finally we conclude the realizability of $\bar{\psi}^{n+1}$.

1. We initialize $\bar{f}_j^n := \bar{M}_j^0(\bar{\psi}^n)$. Using the realizability condition (15), we have $\bar{f}_j^n \in \mathcal{A}_1$.
2. Now let us prove that if for all l , $\bar{f}_{jl}^n \in \mathcal{A}_1$ then $\bar{f}_{jl}^{n+\frac{1}{2}} \in \mathcal{A}_1$. We solve (16) by splitting as described above. In the implicit energy step for the homogeneous system we need to solve

$$A \cdot \bar{f}_{jl}^{n+\frac{1}{2}} = S^n (C_j \bar{f}_j^n)_l, \quad (21)$$

where

$$A = \begin{pmatrix} S^{n+1} & 0_{\mathbb{R}^3} \\ 0_{\mathbb{R}^3}^T & (S^{n+1} + 2\Delta\epsilon^n T^{n+1}) Id_{\mathbb{R}^{3 \times 3}} \end{pmatrix} \text{ and } A^{-1} = \begin{pmatrix} 1/S^{n+1} & 0_{\mathbb{R}^3} \\ 0_{\mathbb{R}^3}^T & 1/(S^{n+1} + 2\Delta\epsilon^n T^{n+1}) Id_{\mathbb{R}^{3 \times 3}} \end{pmatrix}.$$

The right hand side of (21) is realizable, because $C_j \bar{f}_j^n$ is a convex combination of realizable moments. This means that the norm of the second component of $C_j \bar{f}_j^n$ is bounded by the first component (see (5)). Since A^{-1} divides the second component by a bigger value than the first component, this remains true for the vector $\bar{f}_{jl}^{n+\frac{1}{2}}$, which is therefore realizable (according to the characterization (5)).

Then $\bar{M}_{jl}^{n+1} := \bar{f}_{jl}^{n+\frac{1}{2}} \in \mathcal{A}_1$. We eventually obtain $\bar{\psi}_l^{n+1} \in \mathcal{A}_1$ by (20).

□

2.2 Scheme for fast characteristics in 1D

As mentioned above, for a standard scheme the density ρ in front of the flux term might lead to a severe CFL restriction. We overcome this problem by stencil extensions, which rely on a re-interpretation of the basic upwind scheme. For the sake of simplicity we describe this approach first for the 1D linear advection equation. Consider

$$\partial_t u + \frac{a}{\rho(x)} \partial_x u = 0, \quad (22)$$

with $a > 0$ (the case $a < 0$ can be treated similarly).

We consider a fixed mesh. And the time step Δt is a priori independent of mesh size Δx (i.e. not constraint by a CFL condition).

In a basic Finite Difference (FD) framework, we write $u_l^n = u(x_l, t^n)$. And we consider $\rho = \rho_l$ constant in each cell $C_l = [x_{l-\frac{1}{2}}, x_{l+\frac{1}{2}}]$. A scheme is obtained by defining u_l^{n+1} as a convex combination C of some u_i^n such that this definition is consistent with (22).

Using the method of characteristics, u is constant along the characteristic curves. In each cell C_l , this yields $u_l^{n+1} = u(x_l, t^{n+1}) = u(y(\tau, t^{n+1}, x_l), \tau)$ with

$$y(\tau, t, x) = x + \frac{a}{\rho_l}(\tau - t) \quad \text{when } x \in C_l. \quad (23)$$

Now, let us compute the position x_c which the characteristic that goes through $(x_l, t^n + \Delta t)$ reaches at time t^n (see Fig. 1). After computations, one finds

$$x_c = x_{l-k_l+\frac{1}{2}} - c,$$

where

$$c = d \frac{a}{\rho_{l-k_l}}, \quad d = \Delta t - \frac{\Delta x \rho_l}{2a} - \sum_{i=1}^{k_l-1} \frac{\Delta x \rho_{l-i}}{a},$$

and k_l is the number of cell crossed by the characteristic curve. k_l is the only integer verifying

$$\frac{\rho_l \Delta x}{2a} + \sum_{i=1}^{k_l-1} \frac{\rho_{l-i}}{a} \Delta x \leq \Delta t \leq \frac{\rho_l \Delta x}{2a} + \sum_{i=1}^{k_l} \frac{\rho_{l-i}}{a} \Delta x. \quad (24)$$

This configuration is depicted on figure 1.

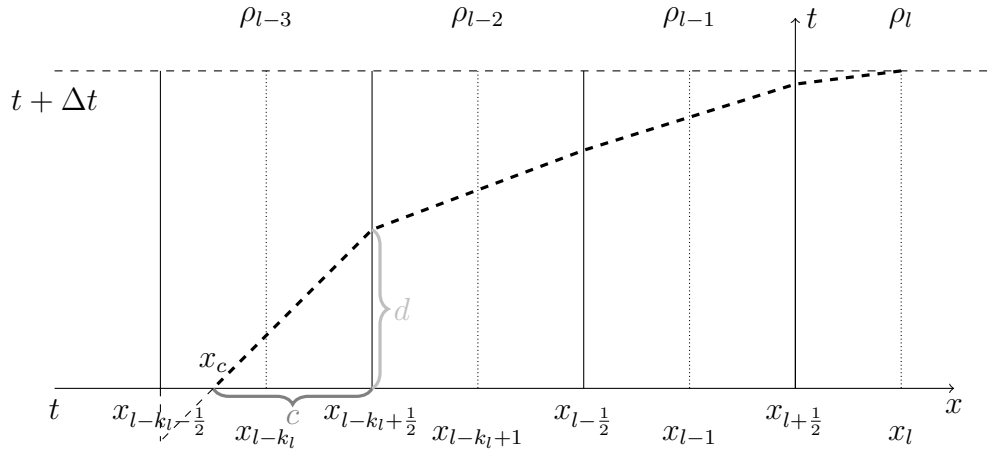


Figure 1. Configuration for CFL-free Finite Difference scheme for $k_l = 3$.

Finally we can compute u_l^{n+1} by interpolation to obtain the following FD scheme

$$u_l^{n+1} = (1 - \alpha)u_{l-k_l+1}^n + \alpha u_{l-k_l}^n \quad \text{if } x_{l-k_l} - x_c \geq 0, \quad (25a)$$

$$u_l^{n+1} = \alpha u_{l-k_l}^n + (1 - \alpha)u_{l-k_l-1}^n \quad \text{if } x_{l-k_l} - x_c < 0, \quad (25b)$$

where

$$\alpha = \left| \frac{x_{l-k_l} - x_c}{\Delta x} \right| = \left| \frac{a\Delta t}{\rho_{l-k_l}\Delta x} - \frac{\rho_l}{2\rho_{l-k_l}} - \sum_{i=1}^{k_l-1} \frac{\rho_{l-i}}{\rho_{l-k_l}} \right| \in [0, 1]. \quad (25c)$$

Remark 1 (Properties of the scheme). • *If the characteristic curves do not cross more than one cell, this scheme is equivalent to the original upwind scheme with the common CFL condition.*

- *The consistency error is $O(\Delta x)$. So it is of order 1 in space and time.*
- *The FD scheme is linear with positive coefficients and whose sum is equal to 1. So it is monotone and therefore Total Variation (TV) stable.*
- *There are no stability restrictions on the scheme, so it is more stable than the common upwind scheme. This allows us to use a bigger time step. But one should keep in mind that the precision obtained when extending the stencil is lower as the one obtained using the common CFL restriction.*

2.3 Extension to multi-D

We study the linear advection equation

$$\partial_t u + \frac{1}{\rho(x)} a \cdot \nabla_x u = 0, \quad (26)$$

where $a \in \mathbb{R}^n$ is a vector and u depends on $x \in \mathbb{R}^n$ and $t \in \mathbb{R}^+$.

For our purposes and in order to simplify the notations, we focus on the two dimensional problem but the method can easily be extended to higher dimensional problems.

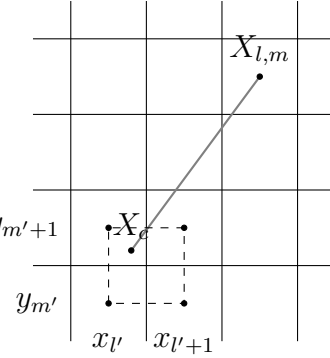


Figure 2. Characteristic for Finite Difference scheme in two dimensions.

Given a cell center $X_{l,m}$, it is straight-forward to find the origin X_c of the characteristic which passes through $X_{l,m}$ at time $t^n + \Delta t$ (cf. Fig. 2). We can then define a Finite Difference scheme by approximating the value of $u_h(X_c, t^n)$ using the values $u_h(\cdot, t^n)$ at the nearest cell centers $X_{l',m'}$ around $X_c = (X, Y)$

$$u_{l,m}^{n+1} = u_h(X_{l,m}, t^n + \Delta t) = u_h(X_c, t^n) \approx \sum_{i=0}^1 \sum_{j=0}^1 \frac{|X - x_{l'+i}|}{|x_{l'+1} - x_{l'}|} \frac{|Y - y_{m'+j}|}{|y_{m'+1} - y_{m'}|} u_{l'+i, m'+j}^n, \quad (27)$$

if $X_c \in [x_{l'}, x_{l'+1}] \times [y_{m'}, y_{m'+1}]$. Coming back to the moment problem, we relax (13) in three

different ways

$$\text{"Cartesian relaxation": directions } \bar{\lambda}_1 = (1, 0), \bar{\lambda}_2 = (-1, 0), \bar{\lambda}_3 = (0, 1), \bar{\lambda}_4 = (0, -1), \quad (28a)$$

$$\text{Associated Maxwellians } \bar{M}_i = \frac{1}{4} \left(\bar{\psi} - \bar{\lambda}_i \cdot \bar{F} \right), \quad \text{for } i = \{1, 4\}, \quad (28b)$$

$$\text{Relaxed system } \partial_\epsilon(S(\epsilon)\bar{f}_i) - \frac{2}{\rho(x)} \bar{\lambda}_i \cdot \nabla_x \bar{f}_i(x, \epsilon) + T(\epsilon)L \cdot \bar{f}_i = \frac{\bar{M}_i(\bar{\psi}) - \bar{f}_i}{\tau} \quad \text{for } i = \{1, 4\}, \quad (28c)$$

$$\text{"Diagonal relaxation": directions } \bar{\lambda}_1 = \frac{1}{\sqrt{2}}(1, 1), \bar{\lambda}_2 = \frac{1}{\sqrt{2}}(-1, 1), \quad (29a)$$

$$\bar{\lambda}_3 = \frac{1}{\sqrt{2}}(-1, -1), \bar{\lambda}_4 = \frac{1}{\sqrt{2}}(1, -1),$$

$$\text{Associated Maxwellians } \bar{M}_i = \frac{1}{4} \left(\bar{\psi} - \bar{\lambda}_i \cdot \bar{F} \right) \quad \text{for } i = \{1, 4\}, \quad (29b)$$

$$\text{Relaxed system } \partial_\epsilon(S(\epsilon)\bar{f}_i) - \frac{2}{\rho(x)} \bar{\lambda}_i \cdot \nabla_x \bar{f}_i(x, \epsilon) + T(\epsilon)L \cdot \bar{f}_i = \frac{\bar{M}_i(\bar{\psi}) - \bar{f}_i}{\tau} \quad \text{for } i = \{1, 4\}, \quad (29c)$$

$$\text{"Star relaxation": directions } \bar{\lambda}_1 = (1, 0), \bar{\lambda}_2 = (0, 1), \bar{\lambda}_3 = (-1, 0), \bar{\lambda}_4 = (0, -1), \quad (30a)$$

$$\bar{\lambda}_5 = \frac{1}{\sqrt{2}}(1, 1), \bar{\lambda}_6 = \frac{1}{\sqrt{2}}(-1, 1), \bar{\lambda}_7 = \frac{1}{\sqrt{2}}(-1, -1), \bar{\lambda}_8 = \frac{1}{\sqrt{2}}(1, -1),$$

$$\text{Associated Maxwellians } \bar{M}_i = \frac{1}{8} \left(\bar{\psi} + \bar{\lambda}_i \cdot \bar{F} \right) \quad \text{for } i = \{1, 8\}, \quad (30b)$$

$$\text{Relaxed system } \partial_\epsilon(S(\epsilon)\bar{f}_i) - \frac{4}{\rho(x)} \bar{\lambda}_i \cdot \nabla_x \bar{f}_i(x, \epsilon) + T(\epsilon)L \cdot \bar{f}_i = \frac{\bar{M}_i(\bar{\psi}) - \bar{f}_i}{\tau} \quad \text{for } i = \{1, 8\}. \quad (30c)$$

Remark 2. • We defined the relaxation directions $\bar{\lambda}_i$, the Maxwellians \bar{M}_i and the relaxed equations so that the stability condition (17), the realizability condition (15) and the consistency condition (14) hold for each set of relaxation parameter.

- When the number of directions J is equal to the number of unknowns (in 2D $\bar{\psi}$ is composed of 3 components), and when the directions are fixed, then the Maxwellians are uniquely defined as a function of $\bar{\psi}$, \bar{F} and of the $\bar{\lambda}_i$. Here, there are more directions in each set (4 in the cartesian and diagonal sets and 8 in the star set) than unknowns, so other choices of Maxwellians may be used.
- All of these schemes are defined using convex combinations. So Propositions 1 hold.

3 NUMERICAL RESULTS

We study several test cases from radiotherapy dose calculation. We use physical values for stopping power and transport coefficient for electrons as described in [1]. The function of interest is the dose defined by

$$D(x) = \int_0^{+\infty} S(\epsilon)\psi^0(x, \epsilon)d\epsilon. \quad (31)$$

In the test case, the dose is normalized by the maximum dose. This normalized dose, called percentage depth dose (PDD) in the field of medical physics, is independent of the quantity of particles transported (which is arbitrary here), it depends only on their distribution.

The following test case was used in [1] to compare the HLL scheme with a Monte Carlo simulation. We consider a domain of size $L_x = 22.3\text{cm} \times L_y = 29.5\text{cm}$, meshed with 223×295 cells. The density in this medium corresponds to a 2D cut of a human chest. We apply a beam modeled by the following boundary conditions

$$(\psi^0, \psi^1) \quad (x = 22.3\text{cm}, y, \Omega, \epsilon) = 10^{10} \exp\left(-\frac{1}{2} \left(\frac{\epsilon_0 - \epsilon}{0.05\epsilon_0}\right)^2\right) \exp\left(-100 \left(y - \frac{L_y}{2}\right)^2\right) \alpha_\mu.$$

Here $\alpha_\mu = (1, \psi^1/\psi^0)$. We choose $\psi^1/\psi^0 = (-0.98, 0)$, it corresponds to an irradiation of the spinal cord. For this test case, $\epsilon_0 = 15\text{MeV}/m_e c^2$. We fix the initial data and the other boundary values with

$$(\psi^0, \psi^1) = (10^{-20}, 0, 0).$$

We compare the solution using a fine energy step $\Delta\epsilon^n = 0.95S^n \left(\frac{1}{\rho_{low}\Delta x} + 2T^n\right)^{-1}$ (HLL scheme) and a coarse one $\Delta\epsilon^n = 0.95S^n \left(\frac{1}{\rho_{water}\Delta x} + 2T^n\right)^{-1}$ using cartesian (28), diagonal (29) and star (30) directions of relaxation. The isodose curves obtained are represented on Fig. 3 in colour over the chest density (grayscale). The isocurves of absolute error induced by the extension of the

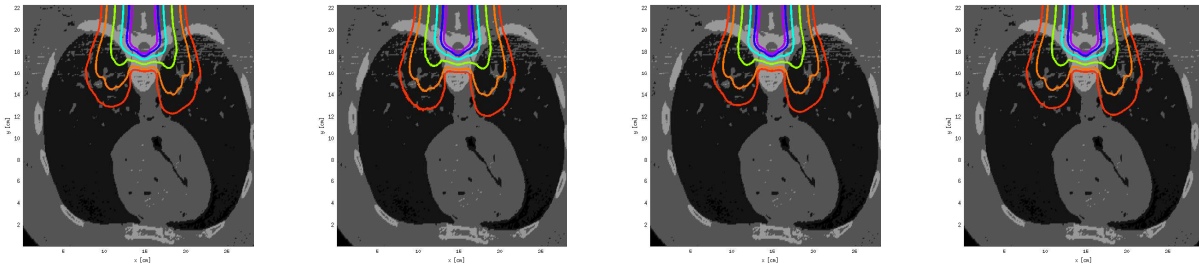


Figure 3. Isodose curves in a chest at 5% (red), 10% (orange), 25% (yellow), 50% (light blue), 70% (dark blue) and 80% (violet) of the maximum dose with a fine $\Delta\epsilon^n$ (left) and a coarse $\Delta\epsilon^n$ using cartesian (middle left), diagonal (middle right) and star (right) directions of relaxation.

stencil normalized by the maximum dose are shown on Fig. 4. The shape of the dose obtained with

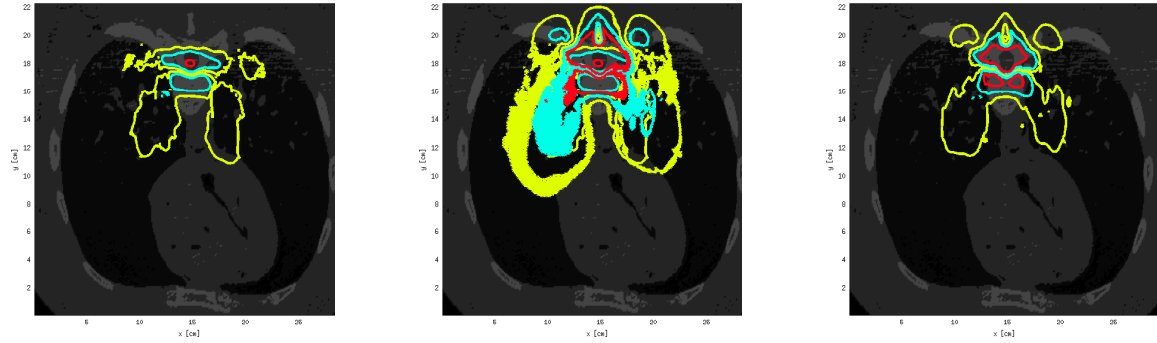


Figure 4. Isocurves of the absolute error between the doses obtained using a fine and a coarse energy step with cartesian (left), diagonal (middle) and star (right) directions of relaxation at 1% (red), 0.5% (light blue) and 0.2% (yellow) of the maximum dose.

the relaxed schemes are very close to the one obtained with the HLL scheme. The absolute error is smaller than 1.1% of the maximum dose when using the cartesian set, smaller than 4.3% with the diagonal set, and smaller than 2.1% with the star set. The maximum errors are located in the middle of the medium at about 2 cm and 6 cm depth. All the voxels are within 3% or 3mm distance-to-agreement for each choice of relaxation parameters. When using the diagonal directions of relaxation, the information is transported in diagonal direction. Then, when transporting particles along the x-axis, the scheme does not transport them from one cell to its neighbor. This results in some irregularities which can be seen in Fig. 4. The relaxed models are better when the directions of relaxation are collinear to the mesh directions (i.e. cartesian directions).

The computation times for this test case are gathered in table I. The numerical schemes pre-

numerical scheme	computation time	number of energy steps
HLL scheme (fine $\Delta\epsilon^n$)	≈ 50 min	146 224
Coarse $\Delta\epsilon^n$ with cartesian set of directions	6.69 sec	460
Coarse $\Delta\epsilon^n$ with diagonal set of directions	7.35 sec	460
Coarse $\Delta\epsilon^n$ with star set of directions	19.72 sec	919

Table I. Computation times for the 2D case with the different schemes .

sented in this paper are significantly faster than the original HLL scheme and gives precise results.

4 CONCLUSION

We have proposed a numerical method for solving the M_1 system of equations applied to radiotherapy dose calculation, which is not constrained by stability restrictions. First, we relax the M_1 system, which leads to a hyperbolic system of equations with linear flux terms. Then, using the method of characteristics, we proposed an inconditionnally stable numerical scheme for hyperbolic systems. This numerical method is equivalent to the HLL scheme when imposing the standard CFL condition. This method was tested on a relevant test case and provides good results

compared to the ones with the HLL scheme, and with a much smaller computational time, as we do not need to impose small energy steps.

5 REFERENCES

- [1] R. Ducloux, B. Dubroca, and M. Frank, “A deterministic partial differential equation model for dose calculation in electron radiotherapy,” *Phys. Med. Biol.*, **55**, pp. 3843–3857 (2010).
- [2] C. D. Levermore, “Moment closure hierarchies for kinetic theories,” *J. Stat. Phys.*, **83**, 5–6, pp. 1021–1065 (1996).
- [3] L. Boltzmann, “Über die mechanische Bedeutung des zweiten Hauptsatzes der Wärmetheorie,” *Wien. Ber.*, **53**, pp. 195–220 (1866).
- [4] E. T. Jaynes, “Information theory and statistical mechanics,” *Phys. Rev.*, **106**, 4, pp. 620–630 (1957).
- [5] D. Kershaw, “Flux limiting nature’s own way,” (1976).
- [6] C. D. Levermore, “Relating Eddington factors to flux limiters,” *J. Quant. Spectrosc. Radiat. Transfer*, **31**, 2, pp. 149–160 (1984).
- [7] A. Harten, P. Lax, and B. V. Leer, “On upstream differencing and godunov-type schemes for hyperbolic conservation laws,” *SIAM Review*, **25**, 1, pp. 35–61 (1983).
- [8] C. Berthon, M. Frank, C. Sarazin, and R. Turpault, “Numerical methods for balance laws with space dependent flux: application to radiotherapy dose calculation,” *Commun. Comput. Phys.*, **10**, 5 (2011).
- [9] D. Aregba-Driollet and R. Natalini, “Discrete kinetic schemes for multidimensional systems of conservation laws,” *SIAM J. Numer. Anal.*, **6**, pp. 1973–2004 (2000).
- [10] D. Aregba-Driollet, R. Natalini, and S. Tang, “Explicit diffusive kinetic schemes for nonlinear degenerate parabolic systems,” *Math. Comp.*, **73**, pp. 63–94 (2004).
- [11] R. Natalini, “A Discrete Kinetic Approximation of Entropy Solutions to Multidimensional Scalar Conservation Laws,” *J. diff. eqns*, **148**, 2, pp. 292–317 (1998).
- [12] F. Bouchut, F. R. Guarguaglini, and R. Natalini, “Diffusive BGK approximations for nonlinear multidimensional parabolic equations,” *Indiana Univ. Math. J.*, **49**, pp. 723–749 (2000).
- [13] F. Bouchut, “Construction of BGK models with a family of kinetic entropies for a given system of conservation law,” *J. Stat. Phys.*, **95**, 1-2, pp. 113–170 (1999).
- [14] B. Dubroca and J. Feugeas, “Hiérarchie des modèles aux moments pour le transfert radiatif,” *C.R. Acad. Sci. Paris*, **329**, pp. 915–920 (1999).